Int. J. Heat Mass Transfer. Vol. 32, No. 11, pp. 2149–2154, 1989
Printed in Great Britain

0017–9310/89 $3.00 + 0.00

The delay time during depressurization of saturated water

A. A. KENDOUSH
Nuclear Research Centre, Iraqi Atomic Energy Commission, P.O. Box 765, Baghdad, Iraq

(*Received* 25 *October* 1988 *and in final form* 10 *March* 1989)

Abstract—The object of this study is to determine the delay time during depressurization after the compressed liquid passes through the saturation state up to the first appearance of detectable bubbles. The experimental range covered starting saturation pressures of 0.33–6.0 MPa. It is shown, experimentally and analytically, that the delay time decreases as the initial saturation pressure of water increases.

1. INTRODUCTION

AN IMPORTANT phase in the thermohydraulic safety design of light water nuclear reactors involves the determination of the water conditions in the various parts of the primary cooling system during depressurization. In the course of system depressurization, subcooled liquid becomes superheated which eventually flash evaporates. There is a finite time between the saturation state of the liquid and the first appearance of detectable bubbles. This time is termed throughout as the 'delay time'. It is a phenomenon that has received little attention in the literature.

Hooper and Abdelmessih [1] carried out depressurization studies in a heated pool of water. They observed a 4–8 ms delay time before the appearance of the first bubble in the liquid. Diffusion of dissolved gas towards bubble nucleation sites is thought by Hanbury and McCartney [2] to be responsible for the delay time. It has been shown [3] that the delay times in pressurized water during blowdown were shorter when water was irradiated with fast neutrons than the non-irradiated water. El-Nagdy and Harris [4] appreciated the existence of the delay time but did not record it quantitatively in their experimental system of neutron induced nucleation.

Weisman *et al.* [5] investigated the initiation of water evaporation on metal surfaces during pressure transients. It was found that, for a water temperature between 90 and 150°C, the wall superheat required to initiate flash evaporation during a rapid pressure transient was significantly higher than required when the pressure was slowly reduced. This result was explained by assuming that a finite time (65 ms–1.6 s) was necessary for vapour to fill the cavity at which the bubble originates. The experimental results of ref. [6] produced delay times up to 11 s at the top of the downcomer pipe during depressurizations of the circulating Freon-113 system.

Skripov [7] believed that metastability, irreversibility and the random nature of the state of superheated liquid are possible causes of the delay time. As part of the nuclear reactor thermohydraulic safety research programme, Edwards [8] studied the flow of flashing liquids in large diameter pipes. The theory and calculations of Edwards were based on the use of an arbitrary value for the delay time. Recently, Siikonen [9] noticed the nonexistence of a theory to predict the delay time during depressurization. Siikonen attributed the failure of the elaborate computer codes, like RELAP5 [10] and K-FIX [11] to model the exact behaviour of reactor coolant during transients, to the inability of these codes to allow for the delay time in their analytical treatment of the flashing process.

The present study produces new experimental and analytical explanations for the delay time encountered during depressurization of saturated and demineralized water.

2. EXPERIMENTAL SYSTEM

A diagram of the system is given in Fig. 1. The depressurization tests were carried out in an electrically heated pressurizer (0.072 m i.d., 2 cm thick and 1 m long). The heaters were mounted on the outside surface of the pressurizer which was surrounded by heat insulators. A displacement pump was used to supply water from a storage tank to the pressurizer through a set of mechanical filters. Downstream of the filters, water either went into the spray nozzles at the vapour region of the pressurizer or into the water region at the bottom of the pressurizer. A high pressure operating needle valve was installed for the control of the water flow in either branch. The water temperature inside the storage tank was measured by a thermocouple. All piping, valves, filters and other fittings were made from stainless steel. The level of water inside the pressurizer was controlled by a special system of valves and a differential pressure transducer. The operational safety of the heaters was ensured by preventing the level of water inside the pressurizer to fall below the level of the heaters. Moni-

NOMENCLATURE

C_p	specific heat at constant pressure
g	gravitational acceleration
h	convective heat transfer coefficient
h_{fg}	specific enthalpy of evaporation
k	thermal conductivity
N	number of microbubbles or bubble nuclei per unit volume
Nu	Nusselt number based on bubble radius, $h(2r)/k$
p	pressure
Pe	Peclet number, $U_g(2r)\rho C_p/k$
Pr	Prandtl number, $\mu C_p/k$
R	gas constant
r	bubble radius
T	absolute temperature
t	time
t_d	delay time
U	velocity.

Greek symbols

α	void fraction
γ	ratio of constant pressure to constant volume specific heat
μ	dynamic viscosity
ρ	density.

Subscripts

f	saturated liquid
g	saturated vapour
sat	saturation
0	conditions at initial depressurization.

toring the temperature of the heaters was done by automatic temperature regulators.

A 5 mCi of gamma rays (type ^{137}Cs) was used for the measurement of the void fraction. The detection of gamma rays was done by an NaI (Tl) scintillation crystal optically coupled to a photomultiplier tube. The centrelines of the gamma source and detector were at a plane 57.9 cm from the bottom of the pressurizer (Fig. 1).

The water temperature inside the pressurizer was measured with a chromel/alumel thermocouple. A Bourdon tube dial gauge was used for pressure monitoring during heating to establish the required initial conditions. A transducer was used for transient pressure measurement. The simultaneous measurement of pressure and temperature during transient allowed the determination of the degree of nonequilibrium in terms of the difference in temperature between that measured and the saturation temperature corresponding to the pressure measurement [6].

A safety valve leading to the vapour region of the pressurizer prevented any unforeseen increase in the

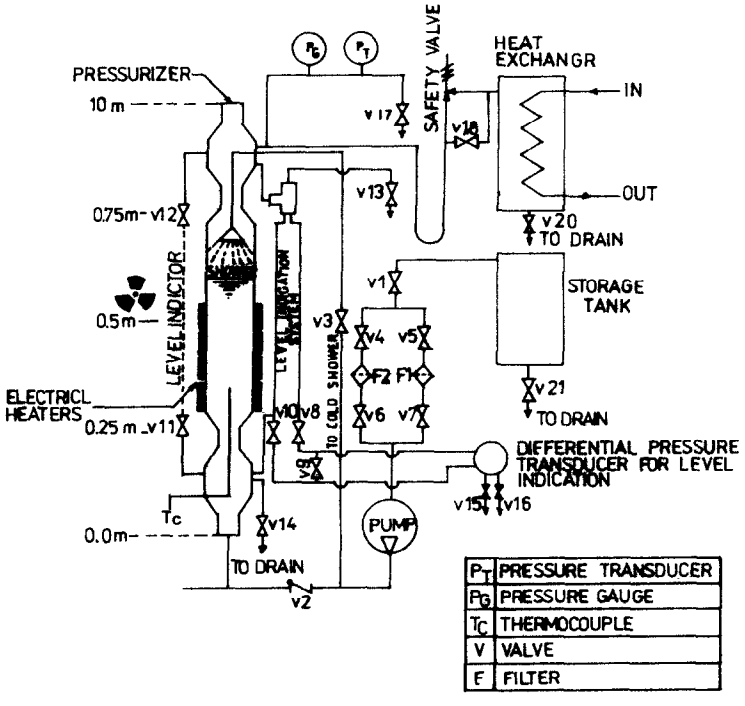

FIG. 1. The experimental system.

pressure. Slow rates of depressurization were initiated by showering a cold water spray into the vapour region of the pressurizer. A heat exchanger was used for the condensation of the steam leaving the pressurizer in the fast depressurization tests. All measuring signals were registered continuously with a multichannel galvanometer recorder which gives a visual display on a u.v. sensitive paper.

2.1. *Depressurization by steam off-take*

The water was raised to the top of the pressurizer allowing all air to go out of the system. Then the system was pressurized under cold conditions to about 25% above the pressure at which depressurization was to initiate, then the system was examined and any leaks were rectified.

Heat was applied up to the saturation conditions where the upper region of the pressurizer was occupied by vapour and the lower region by water. Fast rates of depressurization were effected through the sudden opening of valve V18 in Fig. 1 and allowing the steam to escape to the heat exchanger. Valve V18 is 2.61 m from the centreline of the pressurizer. The range of initial pressures in these depressurizations was 0.33–1.45 MPa.

2.2. *Depressurization by steam condensation*

When the pressure and temperature of the system reached the desired limit, blowdown was initiated by injecting a shower of cold water into the vapour region of the pressurizer. The condensation of vapour causes a decrease in the system pressure. Slow rates of pressure reduction were obtained in these tests. The range of initial pressures investigated was 1.1–6.0 MPa. The displacement pump was used to supply a cold water spray to the pressurizer from the storage tank. Different initial pressures inside the pressurizer produced different rates of flow of the cold water spray. In order to obtain test runs with the same cold water flow rate, it was necessary to calibrate the spray water flow rate against the pump flow rate for different initial pressures inside the pressurizer.

Care was taken in both slow and fast depressurizations to avoid bubble nucleation on the inner heated surface of the pressurizer. This was manifested by switching off the electrical heaters, waiting for the system pressure to fall to the desired initial blowdown value and then starting the run by the injection of the cold shower. In this way, it was anticipated that mainly nucleation of bubbles within the bulk of liquid will be recorded.

3. DELAY TIME THEORY

The phase change from liquid to vapour which is encountered in the system can be represented by the Clausius–Clapeyron equation as

$$\mathrm{d}p = \frac{h_{\mathrm{fg}}}{RT_{\mathrm{sat}}^2} p \,\mathrm{d}T_{\mathrm{sat}} \tag{1}$$

which here includes the perfect gas assumption for the vapour. The transient conditions of the fluid dictates the variation of the pressure (p) and saturation temperature (T_{sat}) with time (t), so

$$\frac{\mathrm{d}p}{\mathrm{d}t} = \frac{h_{\mathrm{fg}}}{RT_{\mathrm{sat}}^2} p \frac{\mathrm{d}T_{\mathrm{sat}}}{\mathrm{d}t}. \tag{2}$$

The depressurization may be considered as an isentropic expansion process, with an initial state of saturated liquid and a final state of fluid just turning into a mixture of vapour and liquid. The final state is at the time where the water temperature starts to depart from the saturation temperature as shown in the experimental results of Fig. 2, hence

$$\frac{T_{\mathrm{sat}}}{T_0} = \left(\frac{V_0}{V}\right)^{\gamma-1} \tag{3}$$

where

$$V = \frac{1}{\rho}$$

and the density of the mixture of vapour and liquid is

$$\rho = \alpha\rho_{\mathrm{g}} + (1-\alpha)\rho_{\mathrm{f}}. \tag{4}$$

Differentiating equation (3) with respect to time yields

$$\frac{\mathrm{d}T_{\mathrm{sat}}}{\mathrm{d}t} = -T_0(\gamma-1)\left(\frac{\rho}{\rho_0}\right)^{\gamma-2}\frac{\rho^2}{\rho_0}\frac{\mathrm{d}(1/\rho)}{\mathrm{d}t}. \tag{5}$$

From equation (4) we obtain

$$\frac{\mathrm{d}(1/\rho)}{\mathrm{d}t} = \frac{(\rho_{\mathrm{f}}-\rho_{\mathrm{g}})}{[\alpha\rho_{\mathrm{g}}+(1-\alpha)\rho_{\mathrm{f}}]^2}\frac{\mathrm{d}\alpha}{\mathrm{d}t}. \tag{6}$$

The delay time (t_{d}) was noticed quantitatively from the experimental results of the void fraction as shown in Fig. 3. In this model, it is postulated that microbubbles start to nucleate at the initial stages of depressurization. Spherical microbubbles of small diameter ($2r$) are formed at their nucleation sites within the liquid. These microbubbles cannot be detected by the available detection means. The number (N) of these microbubbles per unit volume is obtained from

$$\alpha = \tfrac{4}{3}\pi r^3 N \tag{7}$$

and

$$\frac{\mathrm{d}\alpha}{\mathrm{d}t} = 4\pi N r^2 \frac{\mathrm{d}r}{\mathrm{d}t}. \tag{8}$$

The thermodynamic equation for the energy supply from the liquid to provide for the growth of microbubbles can be represented by

$$\frac{\mathrm{d}}{\mathrm{d}t}[(\text{mass of microbubble})\,h_{\mathrm{fg}}] = h(4\pi r^2)(T_{\mathrm{l}}-T_{\mathrm{sat}}). \tag{9}$$

The above equation can be further simplified to obtain

$$\frac{\mathrm{d}r}{\mathrm{d}t} = \frac{h(T_{\mathrm{l}}-T_{\mathrm{sat}})}{\rho_{\mathrm{g}}h_{\mathrm{fg}}}. \tag{10}$$

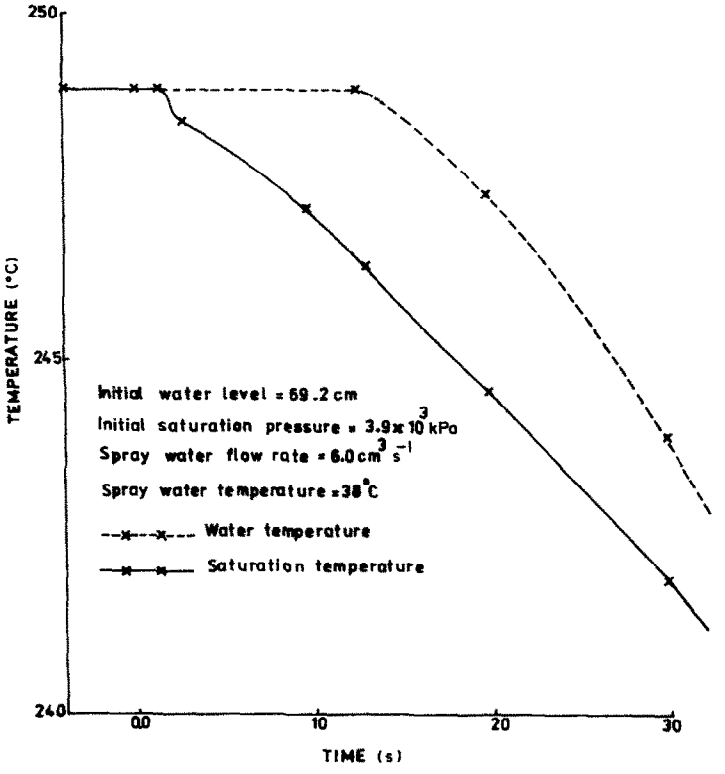

FIG. 2. Variation of the saturation and water temperatures during slow depressurization.

Obviously, thermodynamic nonequilibrium is included in the above equation through the term $(T_l - T_{sat})$. The convective heat transfer coefficient (h) of the microbubble in a swarm was derived on the basis of the cell model and the potential flow as [6]

$$Nu = 1.13\,(Pe)^{1/2}(1-\alpha)^{-1/2} \tag{11}$$

which yields

$$h = 1.13 k_f \left(\frac{\rho_f}{\mu_f}\right)^{1/2} (Pr)^{1/2} \left(\frac{U_g}{2r(1-\alpha)}\right)^{1/2}. \tag{12}$$

Bubble movement effects were incorporated into the analysis by introducing a constant value for (U_g), this being taken as the bubble rise velocity. Performing the following backward substitutions of equation (12) into equation (10), the new equation (10) into equation (8), the new equation (8) into equation (6), the new equation (6) into equation (5) and the new equation (5) into equation (2) gives

$$\int_{p_0}^{p} \frac{dp}{p} = \frac{-(\gamma-1)}{RT_{sat}^2} \left(\frac{\alpha\rho_g + (1-\alpha)\rho_f}{\rho_0}\right)^{\gamma-2} \times \frac{(\alpha\rho_g + (1-\alpha)\rho_f)^2}{\rho_0} \times \frac{14.2(\rho_f - \rho_g) Nr^2 k_f \left(\frac{\rho_f Pr}{\mu_f}\right)^{1/2} (T_l - T_{sat})}{(\alpha\rho_g + (1-\alpha)\rho_f)^2 \rho_g} \times \left[\frac{U_g}{2r(1-\alpha)}\right]^{1/2} \int_0^{t_d} dt \tag{13}$$

with $\rho_0 = \rho_f$. From the definition of the delay time, the following boundary condition was adopted:

at $t = t_d$

$$\alpha \to 0 \quad \text{and} \quad N \to 1 \text{ bubble m}^{-3}. \tag{14}$$

Approximating $\rho_f - \rho_g \approx \rho_f$, using the above condition in equation (13) and putting $\gamma = 1.3$ (for vapour) we obtain

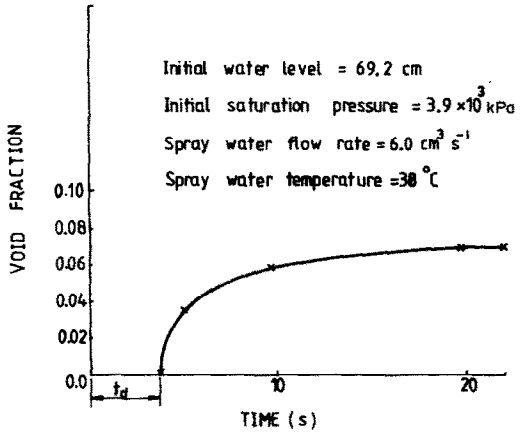

FIG. 3. Evolution of void fraction during depressurization.

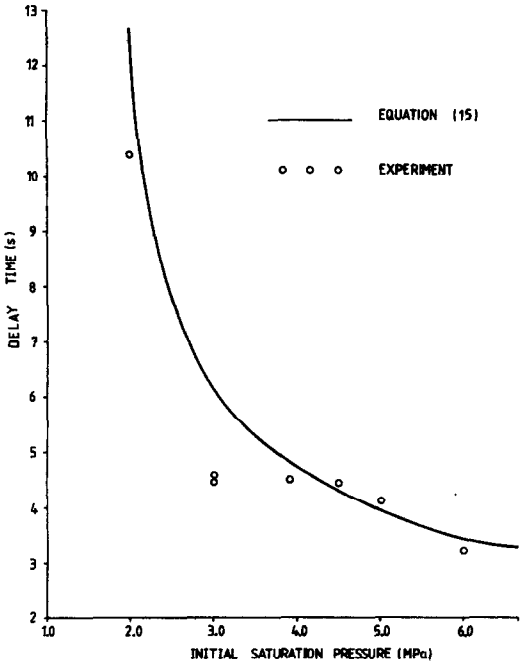

FIG. 4. Prediction of the delay time in the depressurization by condensation tests.

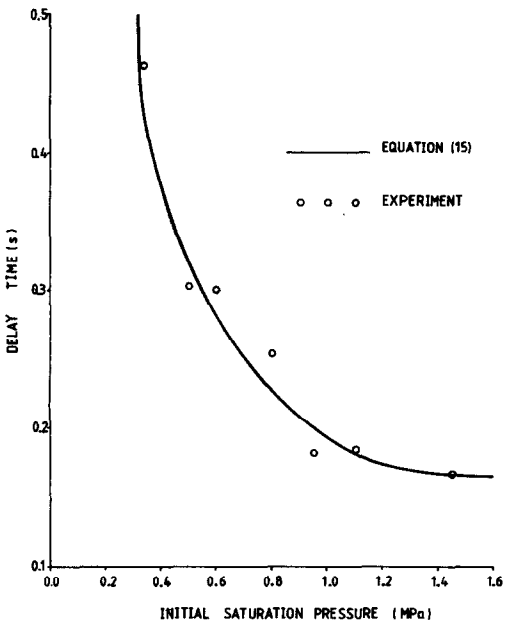

FIG. 5. Prediction of the delay time in the steam off-take tests.

$$t_d = \frac{\ln(p/p_0)}{\psi} \tag{15}$$

where

$$\psi = \frac{-3.01 r^2 k_f}{R T_{sat}^2 \rho_g}\left(\frac{\rho_f Pr\, U_g}{r\mu_f}\right)^{1/2}(T_l - T_{sat}).$$

The constant bubble rise velocity was found to coincide with the ideal bubbly flow region [12], namely

$$U_g = 0.33 g^{0.76}\left(\frac{\rho_f}{\mu_f}\right)^{0.52} r^{1.28}. \tag{16}$$

Assuming a bubble radius of 4×10^{-3} m equation (15) predicted the experimental results of the depressurization by condensation as shown in Fig. 4. The depressurization produced by the steam off-take is envisaged to produce higher bubble rise velocity (within the same region of equation (16)) than the tests of the depressurization by condensation. Keeping the same bubble radius as before, we obtain the prediction of equation (15) to the experimental results of the steam off-take tests as shown in Fig. 5.

4. DISCUSSION OF RESULTS

The system normally reaches the state of saturation and thermodynamic equilibrium before depressurization was initiated. In the course of blowdown, bubble nuclei get activated to produce small size spherical microbubbles. When the system reaches the superheated state, bubbles would have grown in size to the degree that they tend to destabilize the thermal equilibrium of the system. The state of thermal non-equilibrium is clearly shown in Fig. 2, particularly when the saturation temperature falls below the water temperature.

The model proposed in this paper was based on the existence of nonequilibrium in the thermal state of the blowdown fluid. Bubble movement was incorporated in the growth period of the bubble lifetime and an appropriate choice of this movement was used in this model.

Modelling depressurizations of high system pressure particularly related to the water cooled nuclear reactor hypothetical loss of coolant accident (LOCA), dictates the need for the solution of the conservation equations of mass, momentum and energy in order to get the delay time for the flash evaporated coolant which is flowing in the reactor core, piping, safety valves, etc. The pressurizer and any other non-flow components of the primary cooling circuit of the reactor may be modelled according to the methodology reported here.

The comparison between the results of the slow transients of Fig. 4 and the fast transients of Fig. 5, indicates that the former which gives longer delay times than the latter, is more pertinent to the analysis of small break LOCA.

Measurements of the trace displacements on the u.v. trace recording could be made to within ± 0.1 mm which normally represented inaccuracies of the order of $\pm 0.5\%$. Pressure transducer readings were obtained to a high degree of accuracy. There were no significant fluctuations of the trace readings and the estimated accuracy was within $\pm 1\%$, this figure including translation errors from the u.v. recorder.

The random nature of the radioactive decay of the gamma source and the detector dead time produced

signal fluctuations of about ± 1.5 mm in the void fraction data which resulted in an average error of $\pm 2\%$ including translation errors. The careful and accurate calibration and *in situ* checking of the thermocouple made the maximum possible error in the temperature data $\pm 0.16°C$.

5. CONCLUSIONS

Based on the preceding investigation the following conclusions were made.

(1) New experimental and analytical evidence were found for the delay time in flash evaporated water during depressurization.

(2) The delay time decreases as the initial saturation pressure increases.

(3) The inclusion of the delay time in the analysis of small break LOCA may improve the prediction of the pressure, temperature and flow histories of the coolant.

REFERENCES

1. F. C. Hooper and A. H. Abdelmessih, The flashing of liquids at higher superheats, *Proc. 3rd Int. Conf. on Heat Transfer*, Chicago, Illinois (1966).
2. W. T. Hanbury and W. McCartney, Nucleation in the flash boiling of sea water, *4th Int. Symp. on Fresh Water from the Sea*, Vol. 1, pp. 281-291 (1973).
3. A. A. Kendoush, Experiments of neutron induced nucleation, *Nucl. Engng Des.* **110,** 349–360 (1988).
4. M. M. El-Nagdy and M. J. Harris, Experimental study of radiation induced boiling in superheated liquids, *J. Br. Nucl. Energy Soc.* **10,** 131–139 (1970-71).
5. J. Weisman, G. Russel, I. L. Jashnani and H. T. Hsie, The initiation of boiling during pressure transients, ASME Paper No. 73-WA/HT-25 (1973).
6. A. A. Kendoush, Theoretical and experimental investigations into the problem of transient two-phase flow and its application to reactor safety, Ph.D. Thesis, Department of Thermodynamics and Fluid Mechanics, University of Strathclyde, U.K. (1976).
7. V. P. Skripov, *Metastable Liquids*. Wiley, New York (1974).
8. A. R. Edwards, Conduction controlled flashing of a fluid and the prediction of critical flow rates in a one-dimensional system, Report AHSB (S) R-147, United Kingdom Atomic Energy Authority (1968).
9. T. Siikonen, Comparison of flashing heat transfer correlations, 2nd Topical Meeting on Nuclear Reactor Thermal Hydraulics, Santa Barbara, California, January, pp. 11–14 (1983).
10. V. H. Ransom, RELAP5/MOD "O" code description, CDAP-TR-057, E. G. and G. Idaho Inc., U.S.A. (1979).
11. W. C. Rivard and M. D. Torrey, K-FIX: a computer program for transient two-dimensional, two-fluid flow, LA-NUREG-6623, U.S.A. (1977).
12. G. B. Wallis, *One-dimensional two-phase flow*, p. 250. McGraw-Hill, New York (1969).

LE TEMPS-RETARD PENDANT LA DEPRESSURISATION DE L'EAU SATUREE

Résumé—L'objet de cette étude est la détermination du temps-retard pendant la dépressurisation après qu'un liquide comprimé soit passé à travers l'état de saturation jusqu'à l'apparition de bulles détectables. Le domaine expérimental concerne les pressions initiales de saturation d'eau entre 0,33 et 6,0 MPa. On montre, expérimentalement et analytiqument, que le temps-retard diminue quand la pression initiale de saturation croït.

DER ZEITVERZUG BEI DER ENTSPANNUNG GESÄTTIGTEN WASSERS

Zusammenfassung—Gegenstand dieser Untersuchung ist die Bestimmung des Zeitverzugs bei der plötzlichen Entspannung einer zuvor komprimierten Flüssigkeit vom Durchlaufen des Sättigungszustands bis zum Erscheinen der ersten nachweisbaren Blasen. Die im Experiment untersuchten anfänglichen Sättigungsdrücke reichen von 0,33 bis 6,0 MPa. Es wird sowohl experimentell als auch analytisch gezeigt, daß der Zeitverzug mit zunehmendem anfänglichem Sättigungsdruck des Wassers abnimmt.

ВРЕМЯ ЗАПАЗДЫВАНИЯ ПРИ СБРОСЕ ДАВЛЕНИЯ НАСЫЩЕННОЙ ВОДЫ

Аннотация—Целью данного исследования является определение времени запаздывания при сбросе давления после прохождения сжатой жидкостью состояния насыщения до первого появления обнаруживаемых пузырьков. Эксперимент проводится в диапазоне значений начального давления насыщения 0,33–6,0 МПа. Экспериментально и аналитически показано, что время запаздывания уменьшается с возрастанием начального давления насыщения воды.